Geology

Subduction initiates at straight passive margins

F.O. Marques, F.R. Cabral, T.V. Gerya, G. Zhu and D.A. May

Email alerting services	click www.gsapubs.org/cgi/alerts to receive free e-mail alerts when new articles cite this article
Subscribe	click www.gsapubs.org/subscriptions/ to subscribe to Geology
Permission request	click http://www.geosociety.org/pubs/copyrt.htm#gsa to contact GSA

Notes

THE
GEOLOGICAL
SOCIETY
OF AMERICA

Subduction initiates at straight passive margins

F.O. Marques*, F.R. Cabral, T.V. Gerya, G. Zhu, and D.A. May
Institute of Geophysics, ETH-Zürich, CH-8092 Zürich, Switzerland

ABSTRACT

Subduction initiation at straight passive margins can be investigated with two-dimensional (2-D) numerical models, because the geometry is purely cylindrical. However, on Earth, straight margins rarely occur. The construction of 3-D models is therefore critical in the modeling of spontaneous subduction initiation at realistic, curved passive margins. Here we report on the results obtained from gravitationally driven, 3-D thermomechanical numerical models using a visco-plastic rheology and a passive margin with a single curved section in the middle. The models show that the curvature angle β can control subduction initiation: the greater β is, the more difficult subduction initiation becomes. The 3-D thermomechanical models provide an in-depth physical understanding of the processes. Specifically, we find that pressure gradients, arising from density differences between oceanic and continental rocks, drive subduction initiation, and strongly influence the timing. The main difference between straight (cylindrical) and curved margins is that the orientation of the pressure gradient in 3-D is no longer constant, thus producing a horizontal, along-margin component of flow. We thus conclude that the reason for the impedance of subduction initiation is the result of partitioning of the vertical velocity component into a horizontal component, which therefore decreases the effective slab pull. We infer that, although favorable for subduction initiation in a 2-D model, because the estimated force balance is adequate, the pronounced curvature in the southeast Brazilian margin is a likely explanation why subduction initiation is hampered there.

INTRODUCTION

Understanding subduction initiation at a passive margin is a major geodynamic problem, however it remains highly controversial due to the magnitude of force that is estimated as necessary to overcome bending and frictional resistance to initiate subduction (e.g., McKenzie, 1977; Müller and Phillips, 1991). Many solutions have been proposed for this problem: (1) plate rupture within an oceanic plate or at a passive margin (e.g., Müller and Phillips, 1991); (2) sediment loading at passive margins (e.g., Pascal and Cloetingh, 2009); (3) forced convergence at oceanic fracture zones (e.g., Doin and Henry, 2001; Hall et al., 2003; Gurnis et al., 2004; Leng and Gurnis, 2011); (4) tensile decoupling of the continental and oceanic lithosphere due to rifting (Kemp and Stevenson, 1996); (5) Rayleigh-Taylor instability due to a lateral buoyancy contrast within the lithosphere (Niu et al., 2003); (6) water in the lithosphere (Regenauer-Lieb et al., 2001; Van der Lee et al., 2008); (7) spontaneous thrusting of the buoyant continental crust over the oceanic plate (Mart et al., 2005); (8) small-scale convection in the sublithospheric mantle (Solomatov, 2004); and (9) the interaction of thermal-chemical plumes with the lithosphere (Ueda et al., 2008).

Many parameters that can lead to subduction initiation at a passive margin of Atlantic type have been examined in two-dimensional (2-D) numerical modeling (e.g., Cloetingh et al., 1982; Erickson, 1993; Faccenna et al., 1999; Leroy et al., 2004; Mart et al., 2005; Van der Lee et al., 2008; Goren et al., 2008; Burov and Cloetingh, 2010; Nikolaeva et al., 2010, 2011). In particular, the 2-D numerical models of Nikolaeva et al. (2010) showed that the process of spontaneous subduction initiation, driven by gravitational collapse of a passive margin (e.g., Stern, 2002, 2004), is complex and includes two main stages: initial overthrusting of continental crust over oceanic plate, which may eventually evolve into a second stage of self-sustained subduction. Nikolaeva et al. (2011) evaluated the probability of subduction to initiate at the eastern margins of the Americas and concluded that regions of the South American Atlantic margin were the most prone to subduction initiation. Marques et al. (2013) investigated the effects of topographic forcing on subduction initiation, and concluded that the southeast Brazilian margin is the most prone for subduction initiation.

NUMERICAL MODEL

In order to simulate spontaneous subduction initiation by passive-margin collapse, we use a gravitationally driven, 3-D thermomechanical model in which we do not prescribe any plate velocities. In 3-D, the margin geometry is defined by the angles α and β (Fig. 1A): α is the dip of the continent-ocean lithospheric boundary surface, and β is the angle between the trace of the curved section of the margin at the Earth's surface and the z-axis. To avoid introducing effects from other parameters in our models, we kept α constant along the continent-ocean

boundary (Fig. 1A), despite the curved nature of this boundary in the horizontal xz plane. Here we consider that self-sustained subduction initiates (Figs. 1B–1D) when the sinking oceanic slab reaches 200 km depth (e.g., Nikolaeva et al., 2010).

The GSA Data Repository[1] and Zhu et al. (2013) provide a full description of the numerical method used.

MODELING RESULTS

In addition to analyzing the evolution of material composition (which allows visualizing the configurations of the plates over time), we also analyze the model results based on the evolution of temperature, pressure, and velocity.

Model 1 (β = 0°)

The cylindrical model 1 (straight margin, invariant in the z direction [β = 0°]) serves as the reference model used to evaluate the influence of β in the non-cylindrical models 2 and 3. Under the applied conditions, subduction initiates at ~1.215 m.y. along the entire model domain in the z direction (Fig 1B). The model behavior is 2-D, which is expected for a purely cylindrical model.

Model 2 (β = 20°)

Comparison of model 2 (β = 20°) with model 1 shows that, under identical parametric conditions (except for β), subduction initiates later in comparison to the cylindrical model (at ~1.22 m.y. in model 1, and ~1.96 m.y. in model 2). Furthermore, in contrast to model 1, the subduction process varies in the z direction. From the cross sections shown in Figure 2, it is clear that subduction initiates progressively later from the front wall (z = 0 km, at ~1.96 m.y.) to the back wall (z = 200 km, at >2.5 m.y.).

Model 3 (β = 40°)

Model 3 (β = 40°), like model 2, illustrates that subduction initiates later with increasing β (at 1.22 m.y. in model 1, 1.96 m.y. in model 2, and 9.4 m.y. in model 3). Furthermore, in contrast to models 1 and 2, in which subduction initiated across the entire model (although later with increasing z values in model 2), there

---

*Current Address: Geology Department, University of Lisbon, 1749-016 Lisbon, Portugal; E-mail: fomarques@fc.ul.pt.
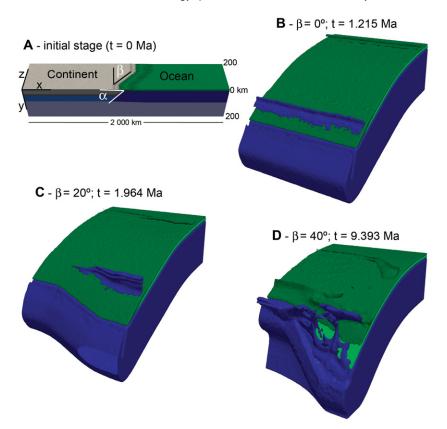

Figure 1. Initial stage (A) and final results (B–D) of modeling. Initial stage shows zig-zag structure to simulate curved margins, lengths of continent and ocean, and angles α and β. α is dip of continent-ocean lithospheric boundary surface, and is 45° for all models; β is angle between trace of curved section of margin at Earth's surface and z-axis, and is 0° (model 1 in B), 20° (model 2 in C), or 40° (model 3 in D). t—time to subduction initiation.
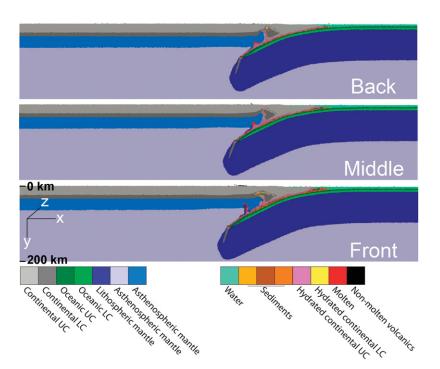

Figure 2. Sections through end result (at 1.964 m.y.) of model 2 with β = 20°, at z = 0 km (front wall), z = 100 km (middle), and z = 200 km (back wall). Note that oceanic slab reaches 200 km depth (subduction proper) faster in front than in back. UC—upper crust; LC—lower crust

was no subduction initiation in the back half of model 3 (Fig. 3).

Temperature, Pressure, and Velocity

The temperature distribution (Fig. DR1 in the Data Repository) shows that the core of the sinking oceanic slab thermally equilibrates over time with the surrounding mantle by becoming hotter. The pressure distribution in advanced stages of subduction initiation is complex, with both vertical and horizontal gradients being present along the margin. The main peculiarity of the curved margin is that horizontal pressure gradients along the z direction are present—a feature that is not present in the cylindrical model. The velocity field in the xy section is rather simpler, with the development of a prominent clockwise vertically elongated convection cell at the continent-ocean boundary. This flow field is a persistent feature from the earliest stages of deformation (Fig. 4).

DISCUSSION

In order to understand the driving mechanism and interpret the different model results, we need to discuss (1) temperature, (2) density gradients, and (3) velocity fields.

Temperature

Temperature is a critical parameter because it controls density, thus affecting stresses and pressure gradients. In the initial stage, isotherms are horizontal, but this configuration rapidly changes with deformation (Fig. DR1). If subduction initiation is fast, as in models 1 and 2, then thermal re-equilibration of the sinking slab with the surrounding mantle is delayed. Hence, the slab remains cold to great depths, the density contrast with the mantle is maintained (cold slab in hot mantle), and the oceanic slab thus sinks rapidly. There is, therefore, a positive feedback between temperature and the sinking velocity of the oceanic slab (e.g., McKenzie, 1977), which can be further enhanced if the cold oceanic slab transforms into high-density eclogite (not modeled).

On the contrary, if subduction initiation is slow, as in model 3, then thermal re-equilibration is promoted. This results in the sinking slab increasing in temperature, the density contrast with the surrounding mantle decreasing (hot slab in hot mantle), the negative buoyancy vanishing, and the oceanic slab sinking more slowly. Such a negative feedback can be further enhanced by the inhibition of eclogite formation. Ultimately, self-sustained subduction may never form; instead, continental overthrusting will develop.

Pressure and Velocity

In order to discuss the pressure and pressure gradients within the models, we need to: (1) evaluate horizontal density gradients in the x and z directions, which produce horizontal pressure gradients at the margin; (2) examine the
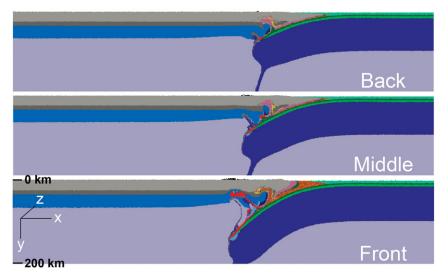
Figure 3. Sections through end result (at 9.393 m.y.) of model 3 with β = 40°, at z = 0 km (front wall), z = 100 km (middle), and z = 200 km (back wall). Note that oceanic slab reaches 200 km depth (subduction proper) in front of model, but not in back. Colors are as in Figure 2.
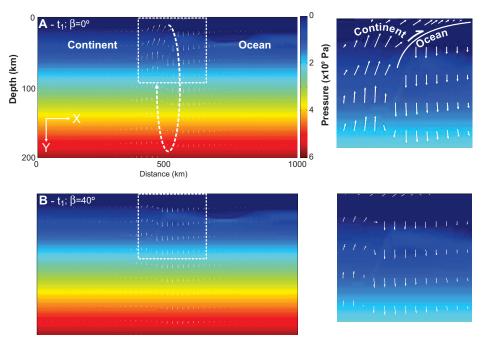

Figure 4. Velocity vectors (white arrows) overlain on pressure maps (colored). The difference in the size of velocity vectors in A (bigger) and B (smaller) indicates why an increase in β hampers subduction initiation. Insets on right are close-ups of the dashed square areas marked in A and B.

velocity vectors to visualize the flow patterns resulting from pressure gradients (Fig. 4); and (3) examine the temperature field (Fig. DR1) because it has a critical effect on density, and an inverse exponential control on the viscosity (the higher the temperature, the lower the viscosity).

It is critical to analyze the density field, as the gradients in density produce horizontal stresses and pressure gradients. In the initial stage: (1) a vertical column on the continental side of the continent-ocean boundary comprises 33 km of upper continental crust (2700 kg m^{-3}), 12 km of lower continental crust (2900 kg m^{-3}), and 35 km of subcontinental mantle (3250 kg m^{-3}); (2) a vertical column on the oceanic side consists of 3 km of water (1000 kg m^{-3}), 8 km of oceanic crust (3100 kg m^{-3}), and 77 km of sub-oceanic mantle (3300 kg m^{-3}). These values imply that, between 0 km and ~20 km depth, the pressure is higher on the continental side,

and below 20 km depth the pressure is higher on the oceanic side. Therefore, the horizontal density gradient in the initial stage generates a pressure gradient (larger on the continental side above 20 km depth), which triggers a clockwise convection cell with flow directed from the continent to ocean above 20 km depth (overthrusting), and from the ocean to the continent below 20 km depth (underthrusting) (Fig. 4).

The pressure distribution described above is similar within the initial stages of all three models presented here. However, there are significant differences regarding the magnitude and orientation of the velocity vectors. In model 1, the z component of velocity is approximately zero, therefore we only have to analyze the interplay between the x and y components in favoring or hampering the process of subduction initiation. In model 1 (faster subduction initiation; Fig. 4A), the velocity vectors in the xy plane show greater magnitude and a greater y component than in model 3 (much slower subduction initiation; Fig. 4B). This increased vertical component of velocity accounts for the faster sinking of the oceanic slab, and thus explains in part the faster subduction initiation. However, in a 3-D model, one has to consider the z component of the velocity vector. The downward pull (y component) can be reduced by having to share part of its magnitude with a horizontal z component (the third dimension being absent in a cylindrical or 2-D model). This is visible on the xz plots of the 3-D velocity field (Fig. DR2). The z component of the velocity vector results from the rotation of the pressure gradient in the oblique trace of the passive margin. Therefore: (1) in models 2 and 3, the continent does not thrust toward the ocean as much as in model 1, especially close to the back wall; and (2) in the central oblique part of the margin, the velocity vector increases its z component with increasing β, overthrusting decreases, loading of the oceanic lithosphere decreases, and the slab pull is reduced.

The 3-D geometry we investigated in this work has a natural counterpart in the southeast Brazilian margin. Here the geodynamic setting and the topographic forcing are favorable for subduction initiation (Nikolaeva et al., 2011; Marques et al., 2013). Despite the favorable setting, and geological and geophysical signs of an early stage of continental overthrusting, a fully developed subduction zone has not yet formed. The 3-D models presented indicate that the development of a coherent subduction zone can be hampered by the curved nature of the southeast Brazilian margin.

CONCLUSIONS

From the numerical results, we conclude that the time required for subduction to initiate increases as the curvature of the passive margin

increases. The physical explanations for this behavior are as follows:

- The density contrast between oceanic and continental blocks generates horizontal stresses and pressure gradients that drive flow from continent to ocean in the crust (overthrusting), and from ocean to continent in the mantle (underthrusting).

- In a curved margin, the pressure gradient is no longer exclusively perpendicular to the straight margin, as in a cylindrical or 2-D model. The more complex 3-D pressure gradient shows that the orientation of the pressure gradient in 3-D produces a horizontal z component of flow, which is not present in cylindrical models.

- The faster the oceanic lithosphere sinks in the initial stages, the faster the subduction initiates because of the relationship between velocity and thermal re-equilibration, and therefore density. The faster the sinking, the colder and denser the plate remains relative to the surrounding mantle, which promotes subduction initiation. A minimum velocity is needed to maintain cold isotherms at depth; otherwise temperature increases in the sinking slab. This causes the density contrast between lithosphere and asthenosphere to vanish, thus the oceanic lithosphere becomes buoyant and can no longer initiate self-sustained subduction.

While the southeast Brazilian margin may be favorable for subduction initiation in a 2-D model, because the estimated force balance is adequate (Marques et al., 2013), our 3-D models suggest that the arcuate margin geometry may hinder fast subduction initiation

REFERENCES CITED

Burov, E., and Cloetingh, S., 2010, Plume-like upper mantle instabilities drive subduction initiation: Geophysical Research Letters, v. 37, L03309, doi:10.1029/2009GL041535.

Cloetingh, S.A.P.L., Wortel, M.J.R., and Vlaar, N.J., 1982, Evolution of passive continental margins and initiation of subduction zones: Nature, v. 297, p. 139–142, doi:10.1038/297139a0.

Doin, M.-P., and Henry, P., 2001, Subduction initiation and continental crust recycling: The roles of rheology and eclogitization: Tectonophysics, v. 342, p. 163–191, doi:10.1016/S0040-1951 (01)00161-5.

Erickson, S.G., 1993, Sedimentary loading, lithospheric flexure, and subduction initiation at passive margins: Geology, v. 21, p. 125–128, doi: 10.1130/0091-7613(1993)021<0125:SLLFAS> 2.3.CO;2.

Faccenna, C., Giardini, D., Davy, P., and Argentieri, A., 1999, Initiation of subduction at Atlantic-type margins: Insights from laboratory experiments: Journal of Geophysical Research, v. 104, p. 2749–2766, doi:10.1029/1998JB900072.

Goren, L., Aharonov, E., Mulugeta, G., Koyi, H.A., and Mart, Y., 2008, Ductile deformation of passive margins: A new mechanism for subduction initiation: Journal of Geophysical Research, v. 113, B08411, doi:10.1029/2005JB004179.

Gurnis, M., Hall, C., and Lavier, L., 2004, Evolving force balance during incipient subduction: Geochemistry Geophysics Geosystems, v. 5, Q07001, doi:10.1029/2003GC000681.

Hall, C., Gurnis, M., Sdrolias, M., Lavier, L.L., and Müller, R.D., 2003, Catastrophic initiation of subduction following forced convergence across fracture zones: Earth and Planetary Science Letters, v. 212, p. 15–30, doi:10.1016/S0012 -821X(03)00242-5.

Kemp, D.V., and Stevenson, D.J., 1996, A tensile, flexural model for the initiation of subduction: Geophysical Journal International, v. 125, p. 73–94, doi:10.1111/j.1365-246X.1996.tb06535.x.

Leng, W., and Gurnis, M., 2011, Dynamics of subduction initiation with different evolutionary pathways: Geochemistry Geophysics Geosystems, v. 12, Q12018, doi:10.1029/2011GC003877.

Leroy, M., Dauteuil, O., and Cobbold, P.R., 2004, Incipient shortening of a passive margin: The mechanical roles of continental and oceanic lithospheres: Geophysical Journal International, v. 159, p. 400–411, doi:10.1111/j.1365-246X .2004.02400.x.

Marques, F.O., Nikolaeva, K., Assumpção, M., Gerya, T.V., Bezerra, F.H.R., do Nascimento, A.F., and Ferreira, J.M., 2013, Testing the influence of far-field topographic forcing on subduction initiation at a passive margin: Tectonophysics, v. 608, p. 517–524, doi:10.1016/j.tecto.2013.08.035.

Mart, Y., Aharonov, E., Mulugeta, G., Ryan, W., Tentler, T., and Goren, L., 2005, Analogue modelling of the initiation of subduction: Geophysical Journal International, v. 160, p. 1081–1091, doi:10.1111/j.1365-246X.2005.02544.x.

McKenzie, D.P., 1977, The initiation of trenches: A finite amplitude instability, in Talwani, M., and Pitman III, W.C., eds., Island arcs, deep sea trenches and back-arc basins: American Geophysical Union Maurice Ewing Series 1, p. 57–61.

Müller, S., and Phillips, R.J., 1991, On the initiation of subduction: Journal of Geophysical Research, v. 96, p. 651–665, doi:10.1029/90JB02237.

Nikolaeva, K., Gerya, T.V., and Marques, F.O., 2010, Subduction initiation at passive margins: Numerical modelling: Journal of Geophysical Research, v. 115, B03406, doi:10.1029 /2009JB006549.

Nikolaeva, K., Gerya, T.V., and Marques, F.O., 2011, Numerical analysis of subduction initiation risk along the Atlantic American passive margins: Geology, v. 39, p. 463–466, doi:10.1130/G31972.1.

Niu, Y., O'Hara, M.J., and Pearce, J.A., 2003, Initiation of subduction zones as a consequence of lateral compositional buoyancy contrast within the lithosphere: A petrological perspective: Journal of Petrology, v. 44, p. 851–866, doi:10.1093 /petrology/44.5.851.

Pascal, C., and Cloetingh, S.A.P.L., 2009, Gravitational potential stresses and stress field of passive continental margins: Insights from the south-Norway shelf: Earth and Planetary Science Letters, v. 277, p. 464–473, doi:10.1016/j .epsl.2008.11.014.

Regenauer-Lieb, K., Yuen, D.A., and Branlund, J., 2001, The initiation of subduction: Critically by addition of water?: Science, v. 294, p. 578–580, doi:10.1126/science.1063891.

Solomatov, V.S., 2004, Initiation of subduction by small-scale convection: Journal of Geophysical Research, v. 109, B05408, doi:10.1029 /2004JB003143.

Stern, R.J., 2002, Subduction zones: Reviews of Geophysics, v. 40, 1012, doi:10.1029/2001RG000108.

Stern, R.J., 2004, Subduction initiation: Spontaneous and induced: Earth and Planetary Science Letters, v. 226, p. 275–292.

Ueda, K., Gerya, T., and Sobolev, S.V., 2008, Subduction initiation by thermal-chemical plumes: Numerical studies: Physics of the Earth and Planetary Interiors, v. 171, p. 296–312, doi:10.1016/j .pepi.2008.06.032.

Van der Lee, S., Regenauer-Lieb, K., and Yuen, D.A., 2008, The role of water in connecting past and future episodes of subduction: Earth and Planetary Science Letters, v. 273, p. 15–27, doi:10.1016/j .epsl.2008.04.041.

Zhu, G., Gerya, T.G., Tackley, P.J., and Kissling, E., 2013, Four-dimensional numerical modeling of crustal growth at active continental margins: Journal of Geophysical Research, v. 118, p. 4682–4698, doi:10.1002/jgrb.50357.